ORIGINAL RESEARCH (AR)

DOI: 10.4274/jems.2024.00236

Journal of ETA Maritime Science 2024;12(4):365-376

State Estimation and Control for a Model Scale Passenger Ship using an LQG Approach

Ferdi Çakıcı[1], Ahmad Irham Jambak[2], Emre Kahramanoğlu[3], Ahmet Kaan Karabüber[4], Bünyamin Ustalı[5], Mehmet Utku Öğür[6], Fuat Peri[7], Ömer Sinan Şahin[8], Mehmet Akif Uğur[4], Afşin Baran Bayezit[9]

[1]Yıldız Technical University, Department of Naval Architecture and Marine Engineering, İstanbul, Türkiye
[2]İstanbul Technical University, Department of Mechatronics Engineering, İstanbul, Türkiye
[3]İstanbul Technical University, Department of Marine Engineering, İstanbul, Türkiye
[4]Yıldız Technical University, Department of Control and Automation Engineering, İstanbul, Türkiye
[5]Yıldız Technical University, Department of Mechatronics Engineering, İstanbul, Türkiye
[6]Yıldız Technical University, Department of Civil Engineering, İstanbul, Türkiye
[7]İstanbul Technical University, Department of Naval Architecture and Marine Engineering, İstanbul, Türkiye
[8]Recep Tayyip Erdoğan University Faculty of Maritime, Department of Marine Engineering, Rize, Türkiye
[9]İstanbul Technical University, Department of Shipbuilding and Ocean Engineering, İstanbul, Türkiye

Abstract

Reducing the roll response of ships between irregular waves is an important issue for the operational requirement. This study presents a roll dynamics model for a passenger ship equipped with active fins. In this study, a Kalman Filter was applied to accurately estimate all states from the measurement of total roll motion and roll velocity (based on fins and waves), even in the presence of measurement noise. Synchronously, a linear quadratic gaussian (LQG) controller actively drives the fins to minimize roll motion and velocity by taking the fin amplitude and rate saturations together. Two different sea states were modeled for the simulation purpose. Results demonstrate the success of the state estimation approach and the remarkable potential of the LQG strategy in roll reduction.

Keywords: Roll stabilization, Kalman filter, LQG

1. Introduction

The challenge of managing roll motion on ships in demanding marine environments is crucial for maintaining safety and comfort standards. Excessive ship rolling raises significant concerns. It can create lateral acceleration that hinder the efficiency of crew operations, increase the duration of tasks, and, in severe cases, render the vessel non-functional. Moreover, the pronounced roll motion can induce vertical acceleration that lead to seasickness in both the crew and passengers, thereby affecting their comfort and operational capabilities. For cargo ships transporting delicate goods, like perishable items, excessive rolling can cause damage to the cargo. Additionally, extreme roll angles can limit the operation of vital equipment, an issue of particular importance for naval vessels engaged in tasks such as weapon system operations, deployment and recovery processes, and sonar functionality in warships.

In pursuit of minimizing ship roll, studies for many years have led to the creation of various technologies designed to mitigate roll, including fins, bilge keels, and antirolling tanks, which differ in their motion mechanisms, placement, and weight. In particular, fins, which work based on acceleration and interaction with the surrounding fluid mass, have become a widely adopted solution [1]. They are particularly effective due to their ability to alter the initially symmetric foil into asymmetry by altering its angle, which generates lift and moment that stabilizes the ship.

Address for Correspondence: Ferdi Çakıcı, Yıldız Technical University, Department of Naval Architecture and Marine Engineering, İstanbul, Türkiye
E-mail: fcakici@yildiz.edu.tr
ORCID iD: orcid.org/0000-0001-9752-1125

Received: 17.04.2024
Last Revision Received: 04.09.2024
Accepted: 20.09.2024

To cite this article: F. Çakıcı, et al. "State Estimation and Control for a Model Scale Passenger Ship using an LQG Approach." *Journal of ETA Maritime Science*, vol. 12(4), pp. 365-376, 2024.

Numerous experiments and research projects have been conducted to investigate and improve the efficiency of fins and rudders in diminishing roll motion. These include Sharif et al.'s [2,3] experimental research, Wu et al.'s [4] implementation of a proportional-integral-derivative (PID) control mechanism, and the utilization of artificial neural networks and fuzzy logic controllers in simulation studies by Liut [5] and Liut et al. [6]. Model predictive controllers have been introduced to address non-linear phenomena, for example, dynamic stalls [7,8]. To design roll motion mitigation fins under random beam-sea scenarios, parallel multi-pattern control approaches and applied computational fluid dynamics have been proposed [9,10]. The effectiveness of both PID and Linear Quadratic Gaussian (LQG) controllers in reducing roll and pitch motions was examined by Kim and Kim [11]. Additional developments include control algorithms customized to ship velocity, encounter angles, and wave conditions by Koshkouei and Nowak [12], along with various robust control techniques by Moradi and Malekizade [13]. Further advancements in this field include Hinostroza et al.'s [14] focus on optimal control with environmental disturbances, Li et al.'s [15] adoption of adaptive neural networks, Luo et al.'s [16] modification of the mathematical model for control design, and Huang et al.'s [17] enhancement of hydrodynamic coefficient estimation online. Recent innovations include improved MPC designs by Jimoh et al. [18], Three-degree-of-freedom (3DOF) motion control strategies by Cakici [19], active adaptive fractional-order sliding mode control (FOSMC) by Lee et al. [20], non-linear feedback controller development by Liang et al. [21], Optimal H_∞ controller designs by Taskin et al. [22], and advanced MPC algorithms by Hu et al. [23]. Rezaei and Tabatabaei [24] demonstrated the effectiveness of an adaptive FOSMC for roll motion control, underscoring the advantages of integrating fractional-order derivatives.

The objective of this research is to investigate the application of an LQG controller that integrates state estimations from Kalman Filters (KFs) with linear quadratic regulator (LQR) control. First, all states (roll motions and rates induced by fins and waves) are separated in the time domain using a KF. A full-state feedback controller is then used to reduce the magnitude of the states. This approach aims to optimize the operation of active fins to significantly reduce the roll motion of the ship. A 3-m Gulet model, which is a class of passenger ships, was used in the simulations. The same model also physically exists in the Yıldız Technical University Hydrodynamic Research Laboratory for the experimental validation of control strategies in future works.

The remainder of this paper is summarized as follows: Section 2 discusses the modeling of system dynamics, focusing on the roll motion of a passenger ship with midship fins and the equations governing this motion. Section 3 details the implementation of the LQG control strategy, which integrates a KF for state estimation and LQR to optimize control actions. Section 4 presents simulation results that validate the effectiveness of the control system by comparing scenarios with and without fins. Section 5 concludes the paper by summarizing the research findings, noting significant reductions in roll motion and rate, and proposing future research directions.

2. System Dynamics Modeling

This paper investigates roll-motion reduction through the utilization of one pair of midship fins under the impact of irregular waves on the beams of states 3 and sea state 4. The proactive manipulation of these fins generates a counteractive moment that mitigates the wave-induced roll. The spatial configuration of the fins is illustrated in Figure 1a, and the Gulet model is shown in Figure 1a, b.

Here, the forces exerted by the port and starboard fins are denoted by F_1 and F_2 respectively, while M_4 signifies the total roll moment resulting from fin action. As the ship's roll motion around the *x*-axis transpires, the fins must pivot around the *y*-axis to engender vertical force. Table 1 lists the parameters of the utilized ships and fins.

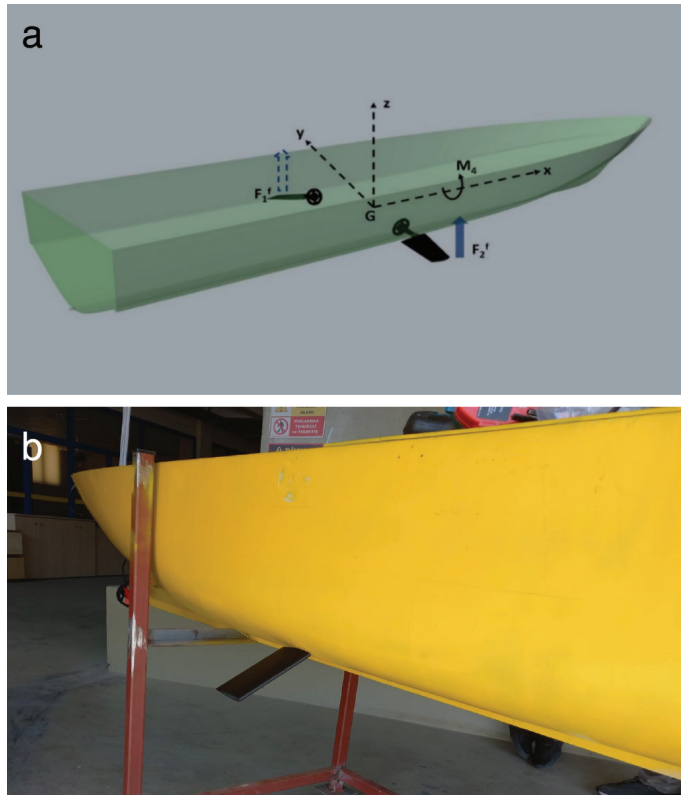

Figure 1. a) *Standard configuration of fins on a ship [25].* ***b)*** *Gulet and fins*

Table 1. *Parameters of the ship and fins*

Parameter	Unit	Value
Waterline length	m	3
Surge speed, *U*	m/s	1.4
Displacement	kg	115.6
Vertical center of gravity (kg)	m	0.30
The transverse metacentric height	m	0.10
Moment of inertia *I*44	kgm^2	6.6
Natural Roll Period	s	1.66
Fin area	m^2	2 x 0.013
Aspect ratio (Span/Chord)	-	2
Moment arm, r_f	M	0.41
C_L (Lift coefficient of the fins)	1/deg	≈ 0.046
K_p (Ship added mass)	kgm^2	0.1997 x I44
K_p (Ship linear damping)	kgm^2/s	4.4

2.1. Passenger Ship Roll Motion Equation

The control system design involves modeling the roll motion dynamics using either a one-degree-of-freedom (1DOF) or complex four-degree-of-freedom (4DOF) approach. For simplicity, the 1DOF model for roll motion was employed as follows (Equations 1 and 2):

$$\dot{\phi} = p \tag{1}$$

$$I_{44}\dot{p} = K_h + K_w + K_c \tag{2}$$

where ϕ, p and I_{44} denote the roll angle, roll velocity (or rate), and moment of inertia about the *x*-axis. K_h encapsulates hydrostatic and hydrodynamic moments, K_w denotes the moment from wave forces while K_c the control moment from the fins. K_h is approximated as follows (Equation 3):

$$K_h \approx K_{\dot{p}}\dot{p} + K_p p + K(\phi) \tag{3}$$

Here, K_p signifies the roll motion added mass coefficient, K_p denotes linear damping coefficient, and $K(\phi)$ denotes the restoring terms generated by gravity and buoyancy forces. Obtaining these coefficients generally involves a combination of experimental measurements, empirical formulas, numerical simulations, and loading conditions, each of which is suitable for capturing different aspects of ship behavior in water.

The term K_w in active control system literature is often omitted due to the complexity associated with the "force superposition method." Instead, this study employs the "motion superposition method", treating ship and wave models separately and combining them to determine the total roll motion and rate [26]. A further exposition of the state space model of the system is provided in the following sections.

2.2. Dynamics of Fin Roll Stabilizer

The investigations into fin stabilizer performances indicate that their effectiveness is reduced under severe sea conditions due to nonlinear effects. In contrast, under milder conditions, the static behavior serves as a sufficient descriptor. Consequently, the focus is placed on the steady behavior of the fins, and the fin-induced roll moment is formulated as [7] (Equation 4):

$$K_c = 0.5\rho r_f V^2 A_f C_L(\alpha_e) \tag{4}$$

where ρ denotes the water density, r_f signifies the roll moment arm, and V represents the relative velocity between fin and flow. A_f, C_L and α_e stand for fin projection area, lift coefficient, and effective angle of attack. The fin section is a NACA 0015 profile, and the aspect ratio (Span length divided by chord length) of the fin is two.

The lift force and angle of attack are linearly related until the stall angle, where the lift force is typically represented as $C_L(\alpha_e) \approx \widetilde{C_L}\,\alpha_e$ with $\widetilde{C_L} \approx \frac{\partial C_L}{\partial \alpha_e}$ at $\alpha_e = 0$. This value was taken as 0.046 (1/deg) for the present fins. The effective angle is calculated as (Equation 5):

$$\alpha_e = -\alpha_{pu} - \alpha_m \tag{5}$$

where α_{pu} is generated by forward velocity and roll rate of the ship while α_m denotes mechanical angle of the fin (Equation 6).

$$\alpha_{pu} = \arctan\left(\frac{V_{roll}}{U}\right) = \arctan\left(-\frac{r_f\dot{p}}{U}\right) \approx -\frac{r_f\dot{p}}{U} \tag{6}$$

Thus, the fins' total roll moments is given by (Equations 7, 8):

$$K_c = K_{cp} + K_{cs} \approx K_\alpha\left(-\frac{r_f\dot{p}-\alpha_m^f}{U}\right) + K_\alpha\left(-\frac{r_f\dot{p}-\alpha_m^{sf}}{U}\right) \quad (7)$$

$$K_\alpha \approx 0.5\rho r_f U^2 A_f \widetilde{C_L} \quad (8)$$

Here, α_m^{pf} and α_m^{sf} represent the mechanical angles of the port and starboard fins, respectively. A schematic of the ship and its fins is shown in Figure 2.

3. Implementation of LQG in Ship Roll Motion Control

The LQG control strategy stands out among control methods due to its effective blend of two key elements: the LQR and the KF. LQR is adept at optimizing control actions to reduce a specific cost function while balancing performance goals and control efforts. In contrast, the KF improves decision making in the presence of noise and uncertainties. The comprehensive LQG controller approach is illustrated in Figure 3.

3.1. Model Derivation for LQG Control

The dynamics of an unforced ship roll can be characterized through a state-space model, where the state equation, as detailed in a numerical study by [25], is described as follows (Equation 9):

$$\dot{\eta}(t) = A_{fin}\eta(t) \quad (9)$$

In this context, the state vector $\eta(t) = \left[\phi_{fin}(t), P_{fin}(t)\right]^T$ comprises the fin generated roll angle $\phi_{fin}(t)$ and the roll rate $P_{fin}(t)$. The system matrix is defined as follows (Equation 10):

$$A_{fin} = \begin{bmatrix} 0 & 1 \\ R & D \end{bmatrix} \quad (10)$$

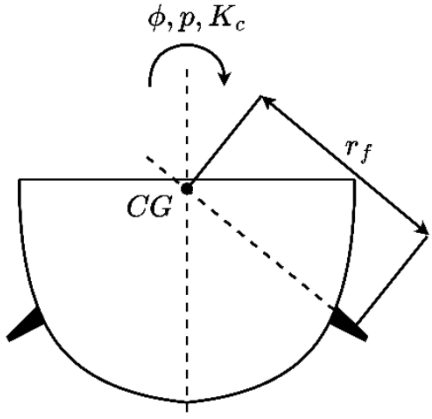

Figure 2. *Representation of ship and fins*

where R and D denote the restoring and damping terms, respectively, which are calculated as follows (Equations 11, 12)

$$R = \frac{-GM_T\Delta}{I_{44}+K_{\dot{p}}} \quad (11)$$

$$D = \frac{-K_p-2K_\alpha r_f/U}{I_{44}+K_{\dot{p}}} \quad (12)$$

This model was adapted to include the effects of ship fins as roll-stabilizing actuators and wave-induced effects. The fin model is integrated using the term B_{fin}, resulting in the following modified ship-motion model (Equations 13, 14):

$$\dot{\eta}(t) = A_{\text{fin}}\eta(t) + B_{fin}u_{fin}(t) + B_{wave}u_{wave}(t) \quad (13)$$

where,

$$B_{fin} = \begin{bmatrix} 0 & 1 \\ \frac{K_\alpha}{I_{44}+K_{\dot{p}}} & -\frac{K_\alpha}{I_{44}+K_{\dot{p}}} \end{bmatrix} \quad (14)$$

Because wave-induced forces are challenging to quantify precisely, the model does not directly incorporate these forces but instead utilizes a motion-based approach encapsulated within the system matrix A_{wave} and B_{wave} as follows (Equation 15):

$$A_{wave} = \begin{bmatrix} 0 & 1 \\ -w_0^2 & -2\zeta w_0 \end{bmatrix}$$
$$B_{wave} = \begin{bmatrix} 0 \\ 2\zeta w_0\sigma \end{bmatrix} \quad (15)$$

where w_0 is the natural frequency and ζ represents the damping ratio of the wave. Please note that the parameters of the A_{wave} matrix is calculated with spectral factorization method with respect to sea state level. A reader interested in the proposed approach can obtain detailed information about the proposed approach [7]. To effectively integrate the ship and wave models, an augmented system is proposed as follows (Equations 16-19):

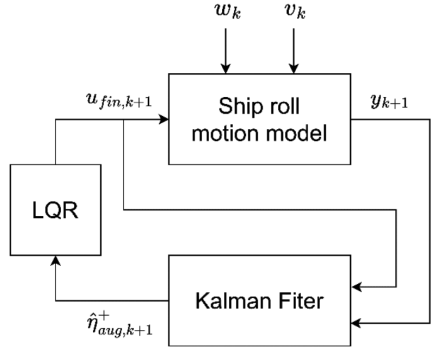

Figure 3. *Flow diagram of an lqg controller for ship roll motion stabilization*

$$\dot{\eta}_{aug}(t) = A_{aug}\eta_{aug}(t) + B_{augf}u_{fin}(t) + B_{augw}u_{wave}(t) \quad (16)$$

$$A_{aug} = \begin{bmatrix} 0 & 1 & 0 & 0 \\ R & D & 0 & 0 \\ 0 & 0 & 0 & 1 \\ 0 & 0 & -w_0^2 & -2\zeta w_0 \end{bmatrix} \quad (17)$$

$$B_{augf} = \begin{bmatrix} 0 & 1 \\ \frac{K_\alpha}{I_{44}+K_{\dot{p}}} & -\frac{K_\alpha}{I_{44}+K_{\dot{p}}} \\ 0 & 0 \\ 0 & 0 \end{bmatrix} \quad (18)$$

$$B_{augw} = \begin{bmatrix} 0 \\ 0 \\ 0 \\ 2\zeta w_0\sigma \end{bmatrix} \quad (19)$$

Here, $\eta_{aug} = [\phi_{fin}(t), P_{fin}(t), \phi_{wave}(t), P_{wave}(t)]^T$ represents the augmented state vector, encompassing both ship- and wave-induced motions and rates.

For digital control systems that operate in discrete intervals, Equation (16) must be discretized (Equation 20):

$$\dot{\eta}_{aug,k} = A_{aug}\eta_{aug,k} + B_{aug}u_{fin,k} \quad (20)$$

Applying the Euler Forward method, the state at the next time step $(k + 1)$ is predicted as follows (Equation 21):

$$\eta_{aug,k+1} = \begin{bmatrix} \phi_{ship,k} + P_{ship,k}\Delta_t \\ P_{ship,k} + \Delta_t(\phi_{ship,k}R + P_{ship,k}D) \\ \phi_{wave,k} + P_{wave,k}\Delta_t \\ P_{wave,k} + \Delta_t(-w_0^2\phi_{wave,k} \pm 2\zeta w_0 P_{wave,k}) \end{bmatrix} + \begin{bmatrix} 0 & \frac{\Delta_t}{} \\ \frac{\Delta_t K_\alpha}{I_{44}+K_{\dot{p}}} & -\frac{\Delta_t K_\alpha}{I_{44}+K_{\dot{p}}} \\ 0 & 0 \\ 0 & 0 \end{bmatrix} u_{fin,k} + \begin{bmatrix} 0 \\ 0 \\ 0 \\ \Delta_t . 2\zeta w_0\sigma \end{bmatrix} u_{wave,k} \quad (21)$$

This leads to the discretized state space representation as follows (Equation 22):

$$\eta_{aug,k+1} = A_{aug,d}\eta_{aug,k} + B_{augf,d}u_{fin,k} + B_{augw,d}u_{wave,k} \quad (22)$$

Where $A_{aug,d}$ and $B_{aug,d}$ denote discretized matrices of A_{aug} and B_{aug} formulated as follows (Equations 23-25):

$$A_{aug,d} = \begin{bmatrix} 1 & \Delta_t & 0 & 0 \\ R\Delta_t & D\Delta_t + 1 & 0 & 0 \\ 0 & 0 & 1 & \Delta_t \\ 0 & 0 & -w_0^2\Delta_t & -2\zeta w_0\Delta_t + 1 \end{bmatrix} \quad (23)$$

$$B_{augf,d} = \begin{bmatrix} 0 & \Delta_t \\ \frac{\Delta_t K_\alpha}{I_{44}+K_{\dot{p}}} & -\frac{\Delta_t K_\alpha}{I_{44}+K_{\dot{p}}} \\ 0 & 0 \\ 0 & 0 \end{bmatrix} \quad (24)$$

$$B_{augw,d} = \begin{bmatrix} 0 \\ 0 \\ 0 \\ \Delta_t . 2\zeta w_0\sigma \end{bmatrix} \quad (25)$$

3.2. Incorporating KF and LQR into LQG Framework

In practical scenarios, models cannot perfectly capture the dynamics of physical systems. Moreover, imperfections in sensor technologies, which result in inaccuracies, limited precision, and stochastic variations, further increase the discrepancies in Equation (21). In this context, the KF is a crucial tool for providing optimal state estimates under these less-than-ideal conditions.

In this study, physical experiments were not conducted. Instead, the true-state measurements were simulated by using the theoretical model established in the previous section. This model is enhanced by incorporating Gaussian process noise to mimic uncertainties that occur in real life. In addition, noise was also added to the measurement model. The complete model is expressed as follows (Equation 26):

$$\left.\begin{aligned} \eta_{aug,k+1} &= A^D_{aug}\eta_{aug,k} + B^D_{augf}u_{fin,k} + B^D_{augw}u_{wave}(t) \\ y_{k+1} &= C\eta_{aug,k+1} + v_k \\ w_k &\sim \mathcal{N}(0, Q_{KF}) \\ v_k &\sim \mathcal{N}(0, R_{KF}) \end{aligned}\right\} \quad (26)$$

Here w_k and v_k represent process and measurement noise, respectively, following Gaussian distributions with covariance matrices Q_{KF} and R_{KF}. The observation C matrix is given as (Equation 27):

$$C = [1 \quad 0 \quad 1 \quad 0; 0 \quad 1 \quad 0 \quad 1] \quad (27)$$

where is the measured total roll motion and rate derived from the combined ship dynamics and wave effect.

The KF state estimation algorithm can be divided into two phases: prediction and estimation. In the prediction phase, the future system state $\hat{\eta}^-_{aug,k+1}$ is computed using the current estimated state $\hat{\eta}^+_{aug,k}$, adjusting (22) as follows (Equation 28):

$$\hat{\eta}^-_{aug,k+1} = A_{aug,d}\hat{\eta}^+_{aug,k} + B_{aug,d}u_{aug,k} \quad (28)$$

The predicted covariance matrix P^-_{k+1} and the Kalman gain $K_{KF,k+1}$ computed as follows (Equations 29, 30):

$$P^-_{k+1} = A_{aug,d}P^+_k A^T_{aug,d} + Q_{KF} \quad (29)$$

$$K_{KF,k+1} = P^-_{k+1}C^T(CP^-_{k+1}C^T + R_{KF})^{-1} \quad (30)$$

Using the $K_{KF,k+1}$, estimated state $\hat{\eta}^+_{aug,k+1}$ and covariance matrix P^+_{k+1} is calculated as follows (Equations 31, 32):

$$\hat{\eta}^+_{aug,k+1} = \hat{\eta}^-_{aug,k+1} + K_{KF,k+1}(y_{k+1}C\hat{\eta}^-_{aug,k+1}) \quad (31)$$

$$P^+_{k+1} = (I - K_{KF,k+1}C)P^-_{k+1} \quad (32)$$

Now that the estimated state from the KF is available, the control input u_k is obtained using LQR, which minimizes the cost function J (Equation 33):

$$J = \sum_{k=0}^{\infty}\left(\eta_{aug,k}^{T} Q_{\text{aug}} \eta_{aug,k} + u_{\text{fin},k}^{T} R_{\text{fin}} u_{\text{fin},k}\right) \tag{33}$$

In the standard LQR framework, the cost function J aims to minimize a combination of the state error weighted by Q and the control effort weighted by R. In addition, $\eta_{\text{fin},k} = \begin{bmatrix}\phi_{\text{fin},k} & P_{\text{fin},k}\end{bmatrix}$ is the state vector for the ship motion. Q_{fin}, R_{fin} are symmetric, positive semi-definite weighting matrices for the state variables and control inputs in each subsystem. The optimal control law for minimizing the cost function J is (Equation 34):

$$u_k = -K_{LQR}\hat{\eta}_{aug,k}^{+} \tag{34}$$

Here, instead of feeding the control law with true state $\eta_{aug,k}$ like typical a LQR control law, $u_{fin,k}$ is computed with the estimated state $\hat{\eta}_{aug,k}^{+}$ obtained from the KF. K_{LQR} is the optimal gain matrix obtained by first solving the following Discrete Algebraic Riccati Equation 35:

$$\mathrm{P} = \mathrm{A}_{\text{aug,d}}^{\mathrm{T}}\mathrm{P}\mathrm{A}_{\text{aug,d}} - \mathrm{A}_{\text{aug,d}}^{\mathrm{T}}\mathrm{P}\mathrm{B}_{\text{aug,d}}\left(\mathrm{R}_{\text{fin}} + \mathrm{B}_{\text{aug,d}}^{\mathrm{T}}\mathrm{P}\mathrm{B}_{\text{aug,d}}\right)^{-1}\mathrm{B}_{\text{aug,d}}^{\mathrm{T}}\mathrm{P}\mathrm{A}_{\text{aug,d}} + \mathrm{Q}_{\text{fin}} \tag{35}$$

Then, K_{LQR} can be calculated as follows (Equation 36):

$$K_{LQR} = \left(R_{\text{fin}} + \mathrm{B}_{\text{aug,d}}^{\mathrm{T}} P \mathrm{B}_{\text{aug,d}}\right)^{-1}\mathrm{B}_{\text{aug,d}}^{\mathrm{T}} P \mathrm{A}_{\text{aug,d}} \tag{36}$$

4. Simulation Results

In this section, the performance of the ship roll stabilization controller is rigorously assessed by simulating its operation under two environmental conditions, specifically, sea state 3 and state 4. These conditions represent moderate and rough sea states, respectively, thus providing a diverse test framework. The simulations were designed to evaluate the controller's ability to maintain stability and effectively respond to varying degrees of wave-induced disturbance. First, the effectiveness of the fins in stabilizing the roll motion of the ship was evaluated. Before these simulations, the effects of active fins were demonstrated in calm water at a 1.4 m/s surge speed while the fins are ±25 degrees and Figure 4 shows the results. As shown in the figure, 4° roll motion is recorded after transition of the response.

The simulation involved two scenarios: one in which the ship was subjected to wave disturbances with passive fins and another in which active stabilizing fins. In the scenario involving active fins, the fin angles were limited to a maximum of ±25 degrees, and the rate of change was capped at ±75 degrees per second. This constraint was implemented to realistically simulate the mechanical limitations of the fins under actual maritime conditions on a model scale. Results from both scenarios were compared to assess the impact of the fins on roll stabilization. Table 2 lists the parameters for sea states 3 and 4. These parameters can be calculated using the spectral factorization method for each sea state. The detailed information about these parameters can be found in [7].

In addition, the KF algorithm was initialized with $Q_{KF} = diag\left([10^{-4}, 10^{-4}, 10^{-4}, 10^{-4}]\right)$ and $R_{KF} = diag\left([10^{-4}, 10^{-4}]\right)$. The simulation length is $50s$ with time step size of $0.02s$. The LQR controller was parameterized differently based on the sea state in which the ship was simulated. Table 3 lists the parameters used to obtain the LQR gain.

Consequently, by solving (35)-(41), the LQR gain matrix for both sea state $K_{LQR,SS3}$ and $K_{LQR,SS4}$ are obtained as follows (Equations 37, 38):

$$K_{LQR,SS3} = \begin{bmatrix}-0.2670 & -1.7160 & -0.2330 & -1.9624\\ 0.2670 & 1.7160 & 0.2330 & 1.9624\end{bmatrix} \tag{37}$$

$$K_{LQR,SS4} = \begin{bmatrix}-0.2687 & -1.6956 & -0.1991 & -1.6304\\ 0.2687 & 1.6956 & 0.1991 & 1.6304\end{bmatrix} \tag{38}$$

It can be observed that variations in the weighting matrices influence the resulting control gains $K_{LQR,SS3}$ and $K_{LQR,SS4}$ which correspondingly exhibit higher and lower gain values. These gain values were employed for controlling in an active fin scenario, and the outcomes were subsequently compared

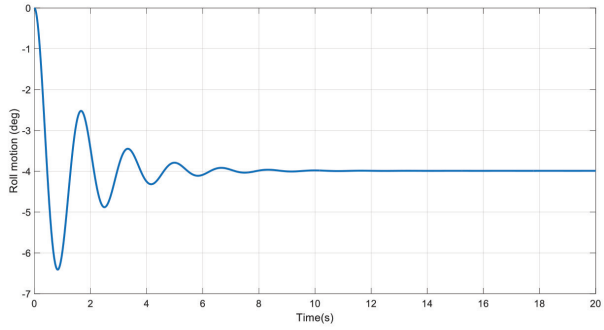

Figure 4. *Demonstration of fins in calm water*

Table 2. *Parameters for sea states 3 and 4*

Parameter	Sea state 3:	Sea state 4:
ζ	0.1603	0.1617
σ	0.1596	0.2678

with those of a passive fin scenario. The comparative results are shown in Figures 5 to 7. The root mean square (RMS) values are detailed in Tables 4 and 5 to quantify the outcomes of the simulation.

In Figure 5, corresponding to the milder sea state 3, the roll motion and roll rate graphs show that active fins, controlled by a more aggressive LQR strategy, significantly reduced the amplitude of roll compared to passive fins. This approach leverages less severe conditions to apply more aggressive control actions that effectively mitigate smaller disturbances and result in smoother, more damped responses. In contrast, Figure 7 where represents rougher sea state 4, where the control strategy is less aggressive but more robust and tailored to cope with larger disturbances typical of harsher sea conditions. Despite the increased severity, the active fins still outperformed the passive fins, maintaining better control over roll motion and rate. Tuning the LQR parameters in sea state 4 aims for durability and sustained performance under

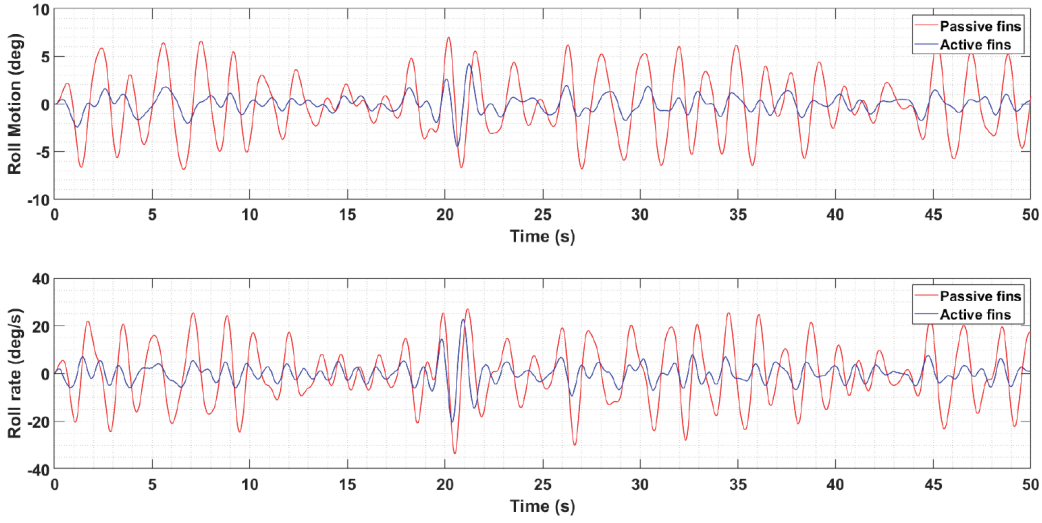

Figure 5. *Comparison of ship roll motion and rate with passive and active fins in sea state 3*

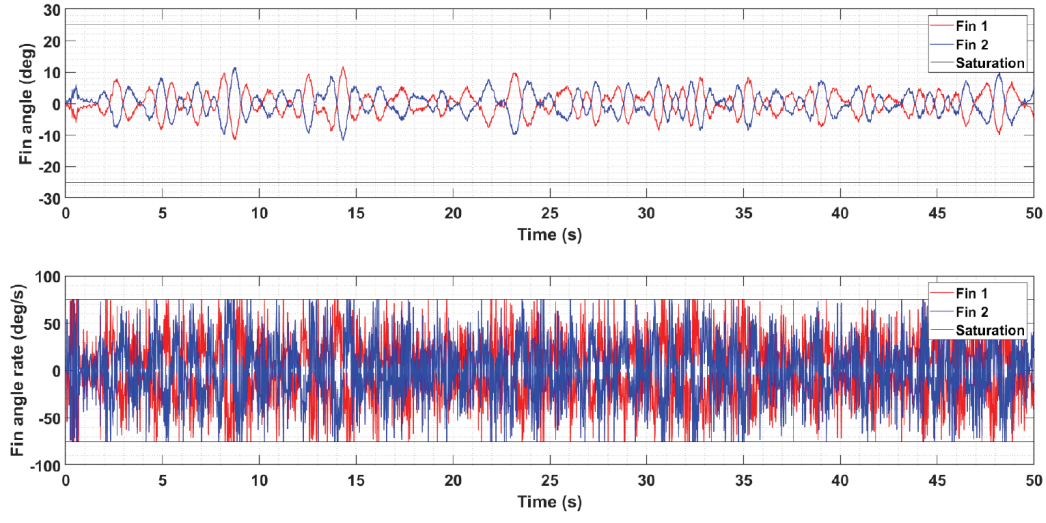

Figure 6. *Fin angular motion and rate in active fin scenario in sea state 3*

Table 3. *LQR parameters*

Parameter	Sea state 3:	Sea state 4:
Q_{fin}	*diag*([1,1])	*diag*([1,1])
Q_{wave}	*diag*([18,18])	*diag*([9,9])
R_{fin}	*diag*([0.1,0.1])	*diag*([0.1,0.1])

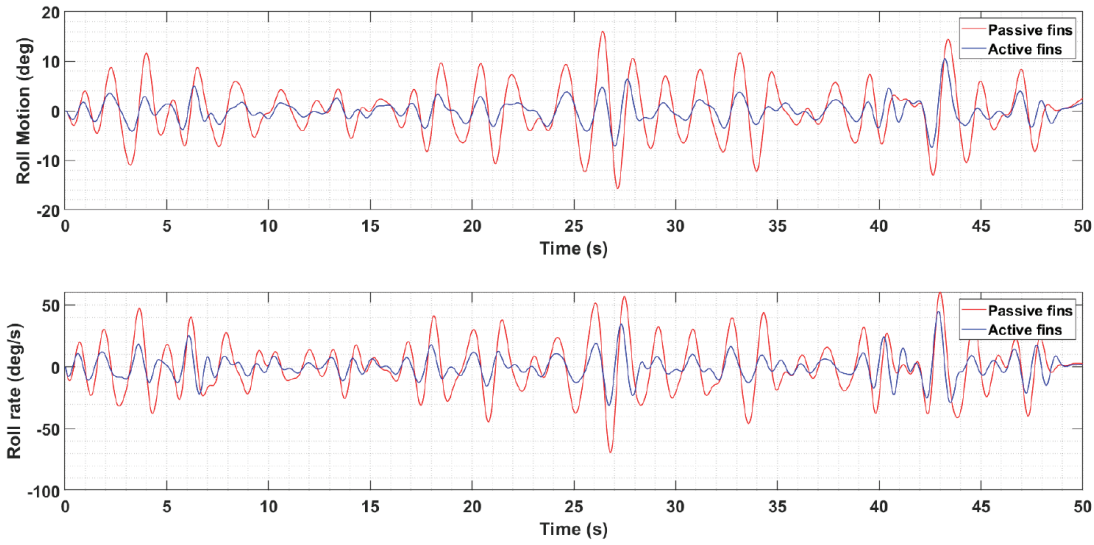

Figure 7. *Comparison of ship roll motion and rate with passive and active fins for sea state 4*

stress, rather than finer control under milder conditions. These findings are further elucidated in Figures 6 and 8, respectively, depict the fin angular motion and rate in sea states 3 and 4, respectively. In sea state 3, fins exhibited higher frequency movements, as indicated by the denser angular rate plot compared to sea state 4. Additionally, in sea state 4, due to harsher conditions, the fins occasionally reached and maintained their maximum angular rate, indicating the struggle as they stabilized the ship's motion.

In Table 4, the reduction percentages for roll motion and rate are quite substantial, at approximately 72.855% and 70.181%, respectively, in sea state 3. This significant reduction underscores the effectiveness of the more aggressive control strategy applied under milder conditions, whereas in Table 5, which presents harsher conditions, the RMS values for both roll motion and roll rate in sea state 4 are higher than those in sea state 3. Despite this, the reductions are still notable, at 57.413% for roll motion and 51.517% for roll rate. Considering the increased environmental challenges, this outcome is satisfactory. The less aggressive, more robust control strategy in sea state 4 is designed not merely to minimize immediate disturbances but to ensure steady and sustained ship stability over time. This approach is particularly important under harsh conditions, where over-reactive control responses can potentially lead to system instability or increased wear and tear on the control mechanisms.

Promising results are observed in Figures 5 and 7, which are quantified in Tables 4 and 5, are controlled based on estimated values $\hat{\eta}^{+}_{aug,k}$ obtained from a KF algorithm, as derived in section 3. KF is crucial because it filters out noise from measurements and compensates for process disturbances, thus providing a refined estimate of the system's state. To validate the reliability and accuracy of these estimates, the KF's performance was validated. The results are presented in Figures 9-12.

However, it is difficult to observe the performance of KF directly, as illustrated in Figures 9 and 11, the overall error in the KF estimation was generally smaller than that in the raw measurements, as shown in Figures 10 and 12. To better understand the performance of KF estimation compared to measurement data with respect to the true value, the RMS values of the errors are presented in Table 6.

Table 6 presents a quantitative assessment of the errors associated with the measured and estimated states for the roll motion and roll rate in sea states 3 and 4, utilizing the KF for the estimation process. The RMS errors for both roll motion and roll rate in sea state 3 indicate a reduction in the error from measurement to estimation, with the roll motion decreasing from 0.576° to 0.437° and the roll rate decreasing from 0.581° to 0.491°. In sea state 4, the results were somewhat consistent, with the roll motion error modestly reduced from 0.579° in raw measurements to 0.442° in estimation.

Table 4. *Roll motion (deg) and rate (deg/s) RMS in sea state 3*

State	Passive fins	Active fins	Reduction (%)
Roll motion	3.053	0.829	72.855
Roll rate	11.926	3.556	70.181

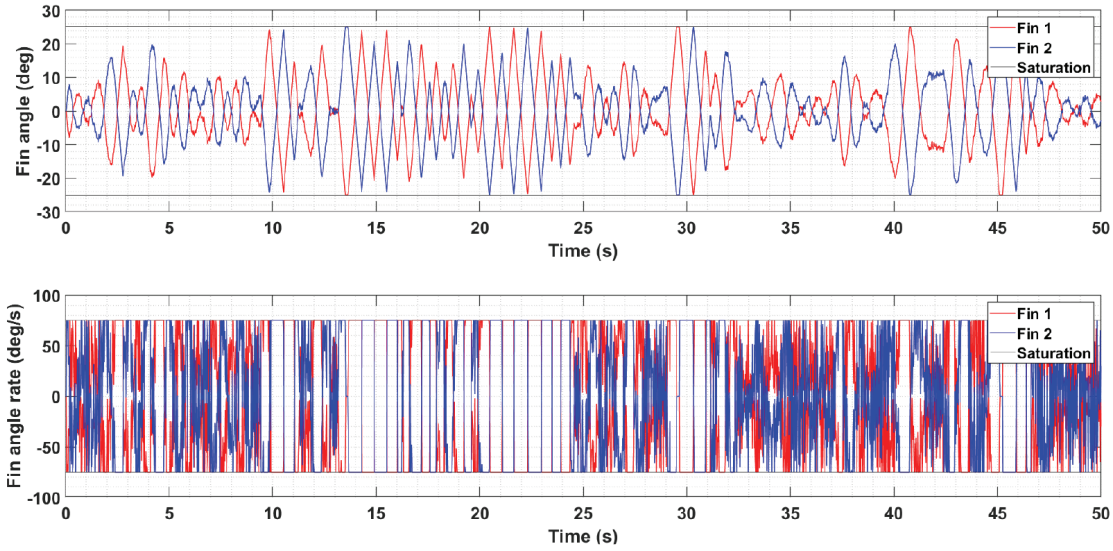

Figure 8. *Fin angular motion and rate in active fin scenario in sea state 4*

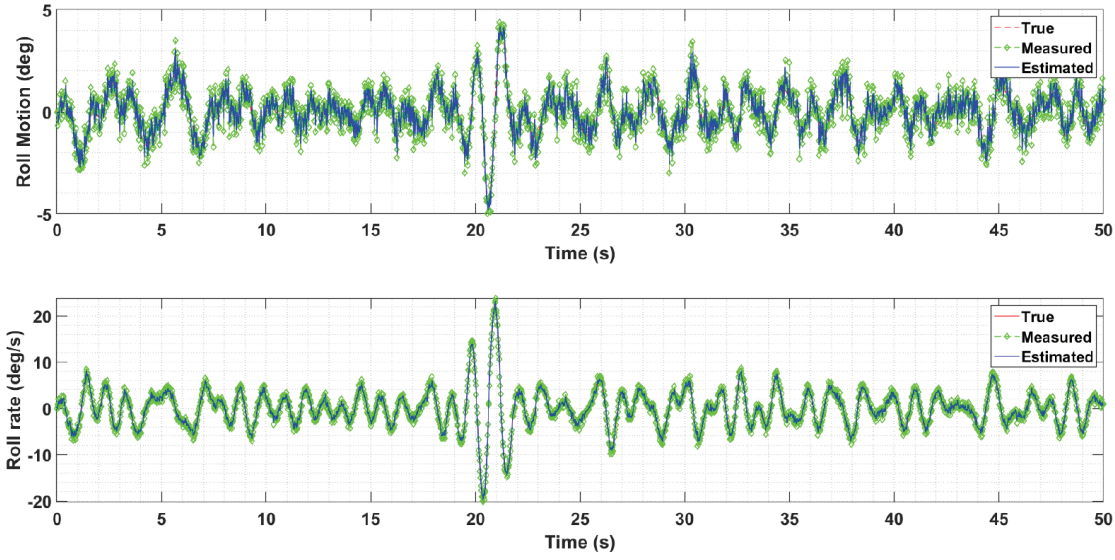

Figure 9. *True, measured, and estimated states in sea state 3 simulation*

Table 5. *Roll motion (deg) and rate (deg/s) of RMS in sea state 4*

State	Passive fins	Active fins	Reduction (%)
Roll motion	5.534	2.356	57.413
Roll rate	21.045	10.203	51.517

Table 6. *RMS of measured vs. estimated roll motion (deg) and rate (deg/s) errors*

	State	Measurement	Estimation
Sea State 3	Roll motion	0.576	0.437
	Roll rate	0.581	0.491
Sea State 4	Roll motion	0.579	0.442
	Roll rate	0.577	0.567

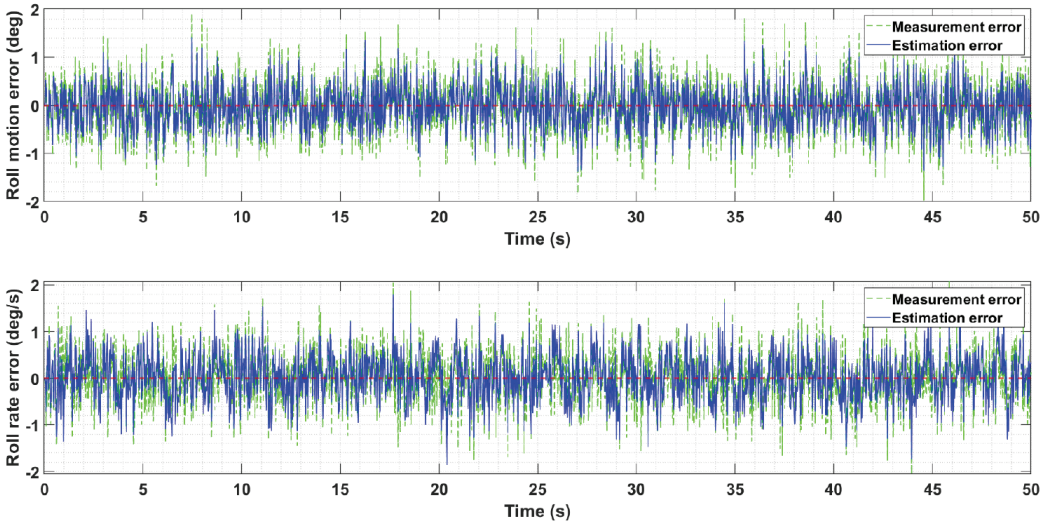

Figure 10. *Measurement and estimation errors in the sea state 3 simulation*

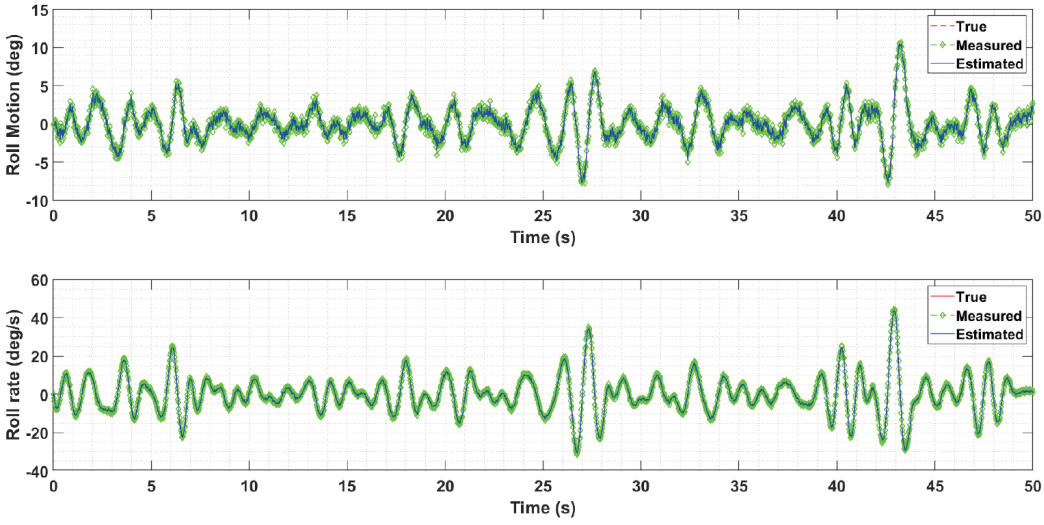

Figure 11. *True, measured, and estimated states in the sea state 4 simulation*

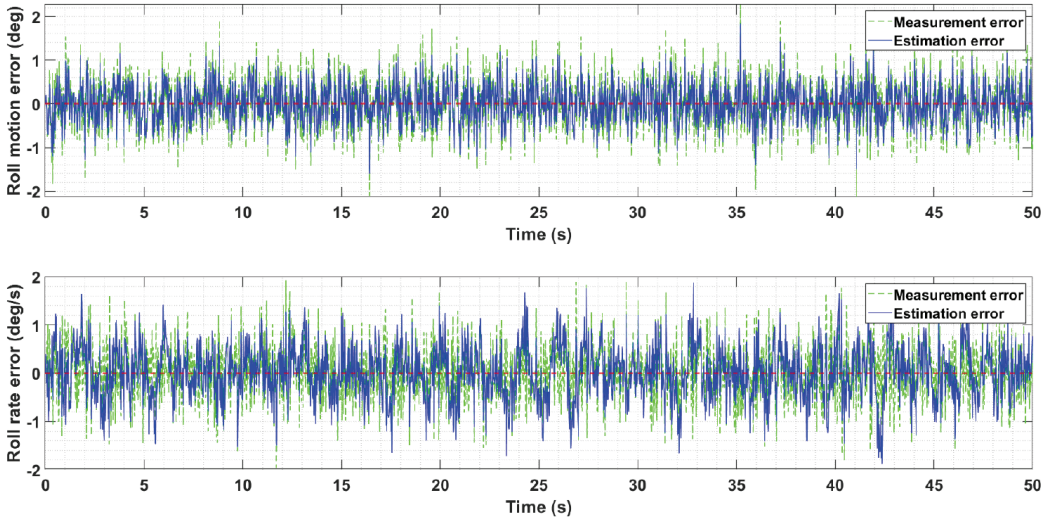

Figure 12. *Measurement and estimation errors in the sea state 4 simulation*

However, the roll rate error exhibits a smaller reduction from 0.577 to 0.567 deg/s. The smaller improvement in roll rate estimation under rougher conditions for sea state 4 might be indicative of the KF reaching its performance limits in more challenging environments.

5. Conclusion

In conclusion, this study successfully demonstrated the effectiveness of an LQG controller for roll motion reduction and its rate of change under wave-disturbed conditions for sea states 3 and 4. The integration of active fins as stabilizers, controlled by the LQG algorithm, led to significant improvements in the vessel's roll response, as evidenced by substantial reductions in roll motion and rate. The accuracy of state estimation through the KF plays a pivotal role in this context, ensuring that the controller inputs are based on precise estimations of the ship's state. This approach provides a more reliable and effective control strategy, highlighting the importance of accurate state estimation in the overall control system design. Furthermore, the results underscore the potential of using advanced control strategies, such as LQG, in marine applications, especially under challenging environmental conditions. This study not only contributes to the field of naval engineering by providing a viable solution for roll stabilization but also sets the groundwork for future research in this area.

Future work could focus on exploring the robustness of this approach under varying sea conditions and ship configurations, as well as integrating real-time environmental data to further enhance the system's adaptive capabilities. In addition, exploring more complex control strategies or integrating other types of stabilizers could provide additional improvements to ship stability and safety.

Footnotes

Authorship Contributions

Concept design: F. Çakıcı, A. I. Jambak, E. Kahramanoğlu, Ö. S. Şahin, A. Baran Bayezit, Data Collection or Processing: F. Çakıcı, A. I. Jambak, A. K. Karabüber, B. Ustalı, M. U. Öğür, F. Peri, M. A. Uğur, Analysis or Interpretation: F. Çakıcı, A. I. Jambak, A. K. Karabüber, M. U. Öğür, F. Peri, Literature Review: A. I. Jambak, A. K. Karabüber, B. Ustalı, M. A. Uğur, Writing, Reviewing and Editing: F. Çakıcı, A. I. Jambak, E. Kahramanoğlu, B. Ustalı, F. Peri, Ö. S. Şahin, M. A. Uğur, A. B. Bayezit.

Funding: This research was supported by the Scientific and Technological Research Council of Türkiye (project number 123M482).

References

[1] J. H. Chadwick, "On the stabilization of roll". *Transactions of the Society of Naval Architects and Marine Engineers*, vol. 63, pp. 237-280, 1955.

[2] M. T. Sharif, G. N. Roberts, and R. Sutton, "Final experimental results of full scale fin/rudder roll stabilisation sea trials". *Control Engineering Practice,* vol. 4, pp. 377-384, Mar 1996.

[3] M. T. Sharif, G. N. Roberts, and R. Sutton, "Sea-trial experimental results of fin/rudder roll stabilisation". *Control Engineering Practice,* vol. 3, pp. 703-708, May 1995.

[4] T. Wu, J. Guo, Y.-N. Chen, and W.-C. Chen, "Control system design and performance evaluation of anti-pitching fins". *Journal of Marine Science and Technology,* vol. 4, pp. 117-122, Dec 1999.

[5] D. A. Liut, *Neural-network and fuzzy-logic learning and control of linear and nonlinear dynamic systems*. Virginia Polytechnic Institute and State University, 1999.

[6] D. Liut, D. Mook, K. Weems, and A. Nayfeh, "A numerical model of the flow around ship-mounted fin stabilizers". *International Shipbuilding Progress*, vol. 48, pp. 19-50, Apr 2001.

[7] T. Perez, *Ship motion control: course keeping and roll stabilisation using rudder and fins*. Springer Science & Business Media, 2006.

[8] T. Perez and G. C. Goodwin, "Constrained predictive control of ship fin stabilizers to prevent dynamic stall". *Control Engineering Practice,* vol. 16, pp. 482-494, Apr 2008.

[9] G. N. Roberts, V. Cournou, B. Vinsonneau, and K. J. Burnham, "Parallel multi-model switched control for ship roll stabilization". *Proceedings of the Institution of Mechanical Engineers, Part M: Journal of Engineering for the Maritime Environment*, vol. 220, pp. 53-65, Jun 2006.

[10] S. Surendran, S. K. Lee, and S. Y. Kim, "Studies on an algorithm to control the roll motion using active fins". *Ocean Engineering*, vol. 34, pp. 542-551, Mar 2007.

[11] J. H. Kim and Y. H. Kim, "Motion control of a cruise ship by using active stabilizing fins". *Proceedings of the Institution of Mechanical Engineers, Part M: Journal of Engineering for the Maritime Environment*, vol. 225, pp. 311-324, Oct 2011.

[12] A. J. Koshkouei, and L. Nowak, "Stabilisation of ship roll motion via switched controllers". *Ocean Engineering*, vol. 49, pp. 66-75, Aug 2012.

[13] M. Moradi and H. Malekizade, "Robust adaptive first–second-order sliding mode control to stabilize the uncertain fin-roll dynamic". *Ocean Engineering*, vol. 69, pp. 18-23, Sep 2013.

[14] M. A. Hinostroza, W. Luo, and C. G. Soares, "Robust fin control for ship roll stabilization based on L2-gain design". *Ocean Engineering*, vol. 94, pp. 126-131, Jan 2015.

[15] R. Li, T. Li, W. Bai, and X. Du, "An adaptive neural network approach for ship roll stabilization via fin control". *Neurocomputing*, vol. 173, pp. 953-957, Jan 2016.

[16] W. Luo, B. Hu, and T. Li, "Neural network based fin control for ship roll stabilization with guaranteed robustness". *Neurocomputing*, vol. 230, pp. 210-218, Mar 2017.

[17] L. Huang, Y. Han, W. Duan, Y. Zheng, and S. Ma, "Ship pitch-roll stabilization by active fins using a controller based on onboard hydrodynamic prediction". *Ocean Engineering*, vol. 164, pp. 212-227, Sep 2018.

[18] I. A. Jimoh, I. B. Küçükdemiral, and G. Bevan, "Fin control for ship roll motion stabilisation based on observer enhanced MPC with disturbance rate compensation". *Ocean Engineering*, vol. 224, 108706, Mar 2021.

[19] F. Cakici, "Vertical acceleration control using LQG approach for a passenger ship". *Ocean Engineering*, vol. 241, 110040, Dec 2021.

[20] S.-D. Lee, S.-S. You, X. Xu, and T. N. Cuong, "Active control synthesis of nonlinear pitch-roll motions for marine vessels". *Ocean Engineering*, vol. 221, 108537, Feb 2021.

[21] L. Liang, Q. Cheng, J. Li, Z. Le, P. Cai, and Y. Jiang, "Design of the roll and heel reduction controller on ship's turning motion". *Ocean Engineering*, vol. 284, 115093, Sep 2023.

[22] M. Taskin, R. Guclu, and A. O. Ahan, "H∞ optimal control of DTMB 5415 combatant roll motion by using active fins with actuator saturations". *Ocean Engineering*, vol. 276, 114255, Mar 2023.

[23] L. Hu, M. Zhang, X. Yu, Z.-M. Yuan, and W. Li, "Real-time control of ship's roll motion with gyrostabilisers". *Ocean Engineering*, vol. 285, 115348, 2023.

[24] A. Rezaei and M. Tabatabaei, "Ship roll stabilization using an adaptive fractional-order sliding mode controller". *Ocean Engineering*, vol. 287, p. 115883, Oct 2023.

[25] F. Cakici, and E. Kahramanoglu, "Numerical roll motion control by using fins based on the linear quadratic regulator and dynamic mode decomposition". *Applied Ocean Research*, vol. 142, 103828, Jan 2024.

[26] T. Perez, and M. Blanke, "Ship roll damping control". *Annual Reviews in Control*, vol. 36, pp. 129-147, Apr 2012.